



Chicken Eggshell Powder as Antibacterial Against *Staphylococcus aureus* and *Escherichia coli* Through *In Vitro* Studies

Rodhiansyah Djayasinga, Rudy Tahan Mangapul Situmeang*, Fuangfa Unob, Sutopo Hadi, Posman Manurung, and Sumardi Sumardi

Received : September 5, 2023

Revised : January 24, 2024

Accepted : January 28, 2024

Online : January 31, 2024

Abstract

Identifying the most effective material with antibacterial properties against *Staphylococcus aureus* (*S. aureus*) and *Escherichia coli* (*E. coli*) is a challenging task considering the rising concerns about drug resistance. Various experiments through *in vitro* and *in vivo* studies to obtain antibacterial agents using abundant and easily available raw material sources have been conducted. Therefore, this study aimed to acquire semiconducting nanoparticle material derived from purebred chicken eggshell waste that could effectively function as an antibacterial agent. The waste treatment was carried out using a top-down method applying the thermal decomposition method with calcination temperatures of 700 and 800 °C for 30 hours. XRD analysis results showed CaO as a major phase and this was further supported by Rietveld calculation. The size of the crystalline phases obtained ranged from 10–45 nm, while FTIR analysis showed the appearance of CaO bond at a wave number of 715.65 cm⁻¹. Furthermore, SEM analysis showed a rough folded particle surface with a pore percentage of 48.20%. Based on the UV-Vis DRS analysis results, chicken eggshell powder had band gap energy characteristics of 2.07, 2.74, 3.71, and 5.96 eV for sample B, as well as 4.60 and 5.82 eV for sample C. Activation of purebred chicken eggshell powder as antibacterial was performed both qualitatively and quantitatively using photocatalytic and non-photocatalytic methods. Qualitatively, both samples showed antibacterial activity, with a minimal inhibitory concentration (MIC) of 1,000 µg/mL.

Keywords: antibacterial, purebred chicken eggshell powder, thermal decomposition, *Staphylococcus aureus*, *Escherichia coli*

1. INTRODUCTION

One of the major public health concerns in various countries worldwide is infectious diseases. Controlling infections caused by pathogenic microbes, which are resistant to antimicrobial drugs, is complicated. Therefore, antibacterial resistance is considered one of the ten most significant global public health threats [1]. Actions to tackle this problem are becoming increasingly important due to the limited available solutions. It is necessary to strengthen efforts aimed at preventing the spread of infectious diseases and develop new drugs to overcome antibiotic resistance [2][3]. Correct and appropriate practices in the use of

antibiotics should also be improved, and self-medication needs to be strictly avoided [4][5].

Staphylococcus aureus possesses the ability to cause infections in humans ranging from mild skin infections to more severe diseases, affecting the heart and lungs [6]. This bacteria may develop resistance to a wide variety of antibiotics previously considered to be effective [7]. Furthermore, *Escherichia coli*, belonging to the Enterobacteriaceae family, can produce extended-spectrum b-lactamase (ESBL) mediated by plasmid enzymes, resulting in resistance to various antibiotics. This bacteria tends to acquire resistance to antimicrobials by evolving through the spread of antibiotic retention genes (ARG) and cellular genetic elements (MGE) among the gene pool [8]-[10].

Several studies have been conducted to find materials capable of preventing infection due to antibacterial resistance, including the use of copper oxide/carbon (CuO/C) nanocomposites synthesized with *Vasica adhatode* leaf extract at room temperature [11], silver and gold-based nanomaterials, zinc oxide, and magnesium ferrite [12]-[15]. Other sources include antimicrobials derived from the hydroethanolic extract of hop

Publisher's Note:

Pandawa Institute stays neutral with regard to jurisdictional claims in published maps and institutional affiliations.



Copyright:

© 2024 by the author(s).

Licensee Pandawa Institute, Metro, Indonesia. This article is an open access article distributed under the terms and conditions of the Creative Commons Attribution (CC BY) license (<https://creativecommons.org/licenses/by/4.0/>).

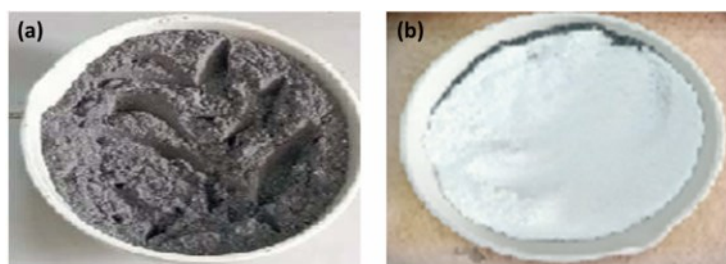


Figure 1. (a) Calcined result of 600 °C and (b) representation of the calcined result.

plants [16][17], shrimp demineralization extract [18], non-specific lipid transfer proteins [19], chicken eggshell [20], and bio-nano composites [21]. Furthermore, various nanomaterials synthesized through chemical, physical, and biological methods using several chemicals have shown antimicrobial properties.

Only a few nanomaterials have been used as photocatalytic antimicrobials, including solvent-cast membranes polyvinylidene fluoride-hexafluoropropylene (Ag-TiO₂/PVDF-HFP) and electrospun membranes Ag-TiO₂/PVDF-HFP. These nanocomposite membranes were tested for antimicrobial activity against liquid culture suspensions of *E. coli* and *Staphylococcus epidermidis*. The test was run using visible light (xenon lamps 600 W/m² at 330 nm) and ultraviolet (8 W UV lamp at 385 nm) with a contact area distance of 18 cm against the suspension of bacteria cells. *E. coli* showed higher susceptibility to death after 90 min of exposure to UV irradiation compared to *S. epidermidis*, as well as during the

300-min experiment using visible light irradiation [22].

Several studies also reported the advantages of antibacterial synthesis from various alternative materials such as curcumin, gelatin, and hydroxyapatite which were further converted into nanocomposites using electrospinning tools for the manufacture of hydroxyapatite-gelatin/curcumin nanocomposites by Sharifi et al [23]. Liu et al. [24] manufactured nanocomposite materials with Cu₂(OH)₂CO₃ composition on the surface of TiO₂ nanoparticles. Motellica et al. [25] explored the synthesis of chitosan/ZnO/Ag nanoparticles/citronella essential oil nanocomposites from ingredients such as silver nitrate, absolute ethanol, Zinc acetate dihydrate, chitosan, glycerol, and acetic acid. However, these methods are associated with complexities and the use of chemicals. The antibacterial activity of CaO powder with a size of 200 mesh from *Anadara granosa* raw material reported by Rusdaryanti et al. [26] gave results capable of functioning as antibacterial with an

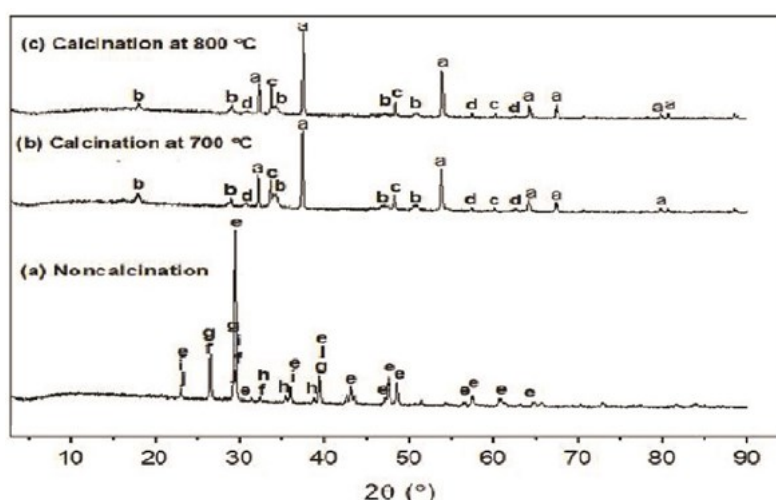


Figure 2. Diffractogram XRD chicken eggshell powder uncalcined, crystal phase calcined at 700 and 800 °C (a) CaO, (b) Ca(OH)₂, (c) CaTiO₃, (d) CuH₄O₆P₂, (e) CaCO₃, (f) P₂O₅, (g) Phosphorus oxynitride (PON), (h) CuO (tenorite), (i) Mg_{0.06}Ca_{0.94}CO₃ (magnesium calcite), and (j) AlCaH₉O₁₃P₂ (overite).

Table 1. Quantitative data of each crystalline phase.

Crystal phase uncalcined	Goodness of Fit (GoF)	2 θ and h k l	FWHM	Particle size (nm)	Weight Percentage of Phase	Crystalline area	Crystalline and amorphous area	Crystalline percentage
CaCO ₃	2.61	29.42 (1 0 4)	0.21	277.54	72.29	2259.34	8110.15	23.75
NOP		26.51 (2 0 1)	0.32	180.99	12.79			
P ₂ O ₅		26.21 (2 0 1)	0.18	321.55	6.54			
Ca _{0.94} Mg _{0.06} CO ₃		29.33 (1 0 4)	0.35	166.49	2.54			
AlCaH ₉ MgO ₁₃ P ₂		23.06 (4 6 0)	0.23	250.15	3.72			
CuO		38.82(1 1 1)	0.19	314.58	2.10			
Crystal phase by calcined at 700 °C	Goodness of Fit (GoF)	2 θ and h k l	FWHM	Particle size (nm)	Weight Percentage of Phase	Crystalline area	Crystalline and amorphous area	Crystalline percentage
CaO	2.17	37.39 (0 0 2)	0.20	41.97	44.96	2228.33	7666.28	29.06
Ca(OH) ₂		34.11 (0 1 1)	0.70	11.88	39.47			
CaTiO ₃		33.64 (0 1 1)	0.18	46.15	9.20			
CuH ₄ O ₆ P ₂		64.26 (1 1 5)	0.23	40.82	6.37			
Crystal phase by calcined at 800 °C	Goodness of Fit (GoF)	2 θ and h k l	FWHM	Particle size (nm)	Weight Percentage of Phase	Crystalline area	Crystalline and amorphous area	Crystalline percentage
CaO	2.28	37.47 (0 0 2)	0.20	41.98	54.84	2265.31	6107.09	37.09
Ca(OH) ₂		34.00 (0 1 1)	0.46	18.07	25.67			
CaTiO ₃		33.88 (0 1 1)	0.70	11.87	11.10			
CuH ₄ O ₆ P ₂		64.29 (3 3 4)	0.30	31.30	8.39			

inhibitory zone of 2.3 mm and a MIC value of 3.5%.

This study only used purebred chicken eggshell waste which could be easily obtained. Chicken eggshell contains 94% calcium carbonate, 1% calcium phosphate, 1% magnesium carbonate, and 4% other organic matters [27][28]. XRF analysis reported that the content (wt%) included CaCO₃ (91.99), MgO (6.79), Na₂O (0.51), P₂O₅ (0.33), Al₂O₃ (0.14), SiO₂ (0.13), K₂O (0.07), Fe₂O₃ (0.04), MnO (0.003), and TiO₂ (0.003) [29]. Based on the literature, the top-down method for preparing CaO nanoparticles from purebred chicken eggshell waste, reported in this study, has not been previously explored. The produced material was also applied as an antibacterial using the irradiation of visible light [30]-[33].

2. MATERIALS AND METHODS

2.1. Bacterial Culture Material

Brian heart infusion broth (BHIB, Merck),

nutrient broth (oxoid), muller hinton agar (MHA, Oxoid), endo agar (Oxoid), mannitol salt agar (MSA, Oxoid), as well as *S. aureus* and *E. coli* were used in this work.

2.2. Chemical Material

The materials used in this study were purebred chicken eggshell obtained from fried rice traders in Bandar Lampung City, Lampung Province, Indonesia, as well as 10% H₂O₂ solution.

2.3. The Instrumentation

X-ray diffraction (XRD-6000 Schimadzu), Fourier-transform infrared (FTIR) (Agilent Technologies Carry 630), scanning electron microscope-EDS (Zeiss EVO MA10), transform electron microscope (Jeo Jem-1400), particle size analyzer (Bacman Coulter), DRS-UV (Cary 60), furnace (Thermolyne), biobase biological safety cabinet (Model BSC-1300IIB2-X), germ incubator (Glotech model GTLI-9082A), porcelain mortar, micropipette, electric scales (BEL Model MW 333i

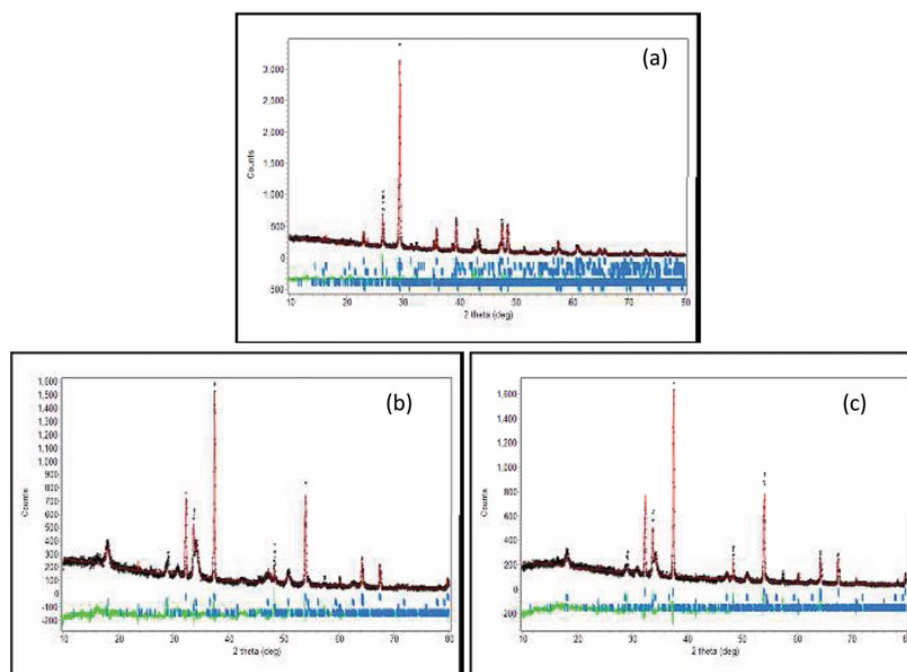


Figure 3. XRD diffractogram of (a) chicken eggshell powder uncalcined and crystal phase calcined at (b) 700 and (c) 800 °C.

type MWnn3i-M), and turbidimeters (Lutron, model TU-2016) were used in this work.

2.4. Manufacture of Eggshell Powder from Purebred Chicken

Purebred chicken eggshell was obtained from fried rice merchant waste in Bandar Lampung area. Samples were ground using mortar until smooth and then calcined at 600 °C [34]. After 15 h, the

calcining process was stopped until room temperature was reached. Calcining was subsequently resumed to the desired temperature (700 and 800 °C) and maintained for 15 h to obtain uniformity of shape and size [35]-[38].

2.5. Bacterial Inoculation and Identification

Preparation of both bacteria and antibacterial susceptibility test of purebred chicken eggshell

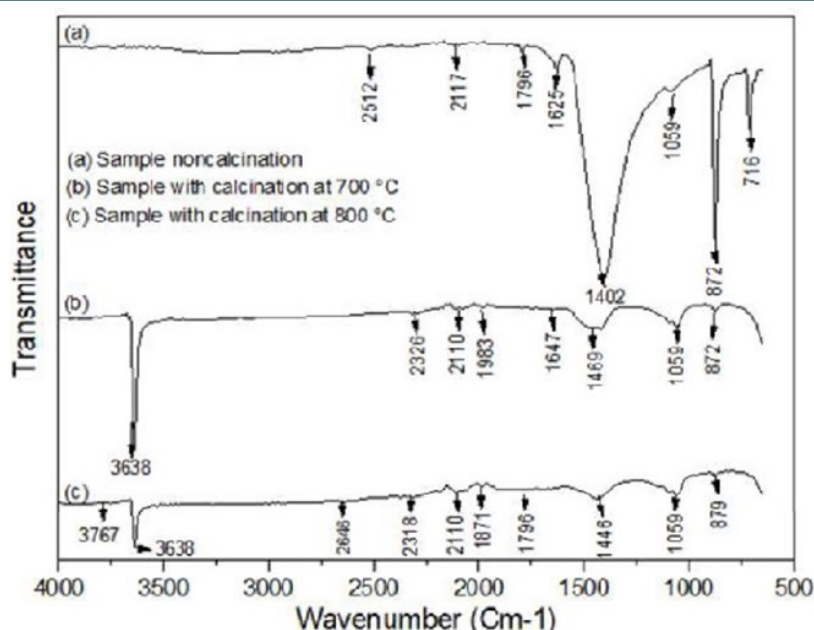


Figure 4. FTIR spectrogram of (a) chicken eggshell powder uncalcined and crystal phase calcined at (b) 700 and (c) 800 °C.

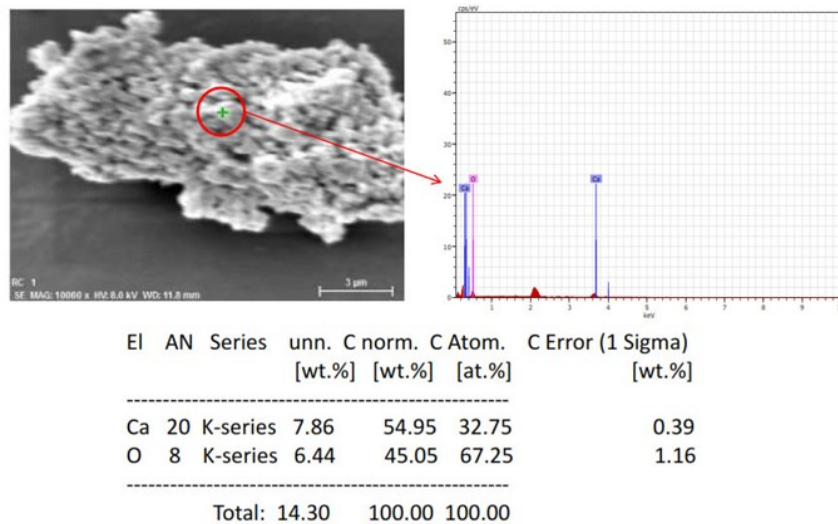


Figure 5. Results of SEM-EDS analysis magnification 10,000× for sample crystal phase calcined at 800 °C.

powder referred to previous studies [39][40]. In this study, *S. aureus* and *E. coli* were sourced from bacteria stocks in the Bacteriology Laboratory at the Tanjungkarang Health Polytechnic Educational Institution, Department of Medical Laboratory Technology, Lampung Province, Indonesia. Both bacteria were inoculated into a liquid culture of BHIB, and incubated at 37 °C for 24 h. *S. aureus* was inoculated again in a MSA culture, while *E. coli* was inoculated in endo agar culture [41]-[43].

2.6. Antibacterial Qualitative and Quantitative Test Against Bacteria

Qualitative tests were conducted by inoculating *S. aureus* and *E. coli* in MHA bacterial cultures. Crystal phase calcined at 700 and 800 °C were then placed on the MHA surface, and both MHA cultures were irradiated by sunlight for 5 min as a photocatalysis technique, and then incubated at 37 °C for 24 h [39]. As a comparison, bacterial inoculation was also carried out in MHA cultures

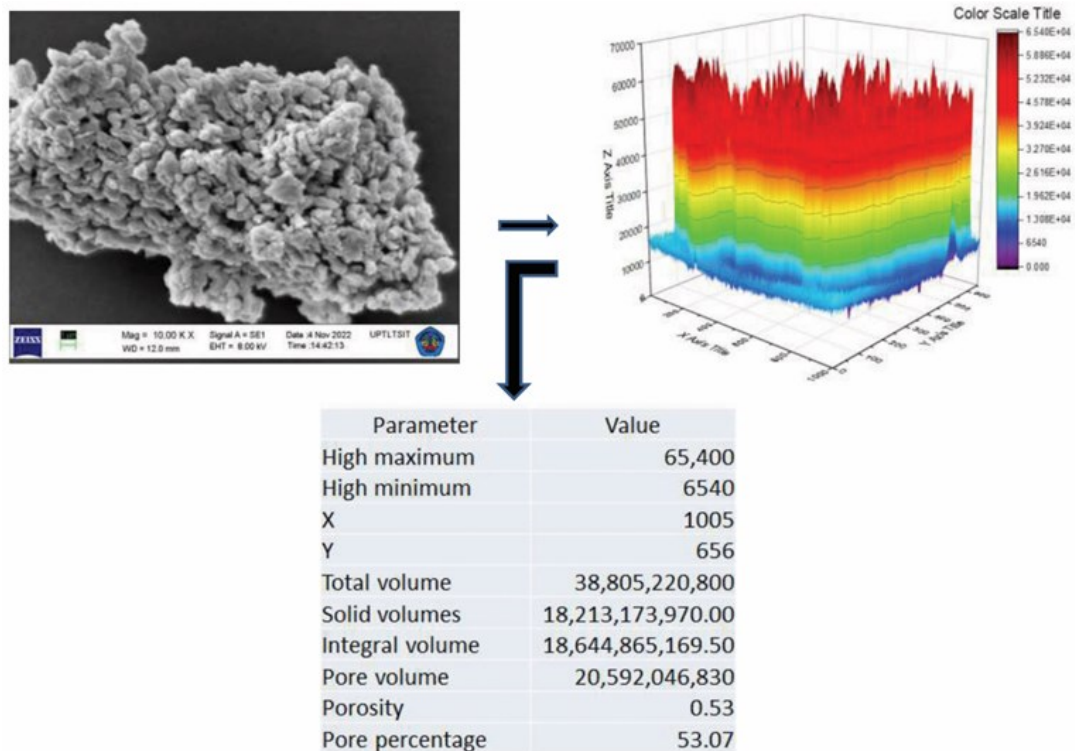


Figure 6. Porosity percentage analysis of SEM micrographs of sample crystal phase calcined at 800 °C.

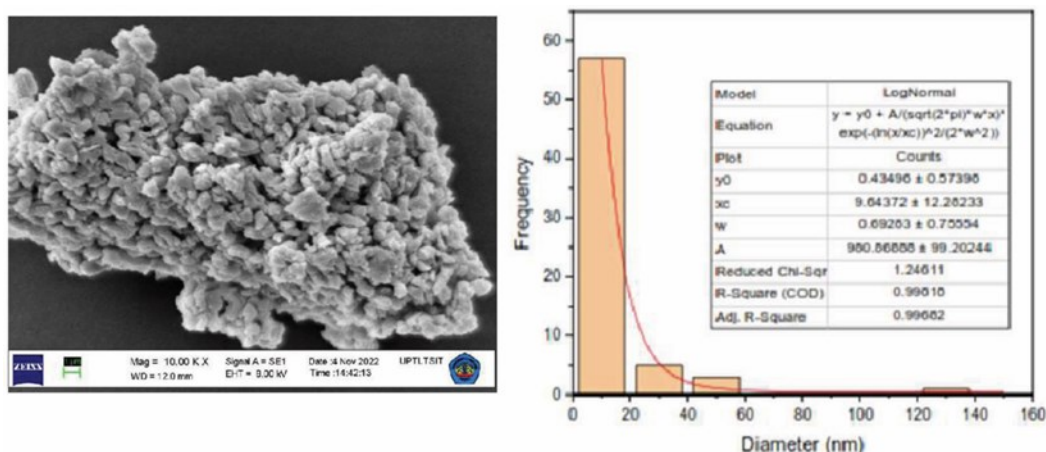


Figure 7. Distribution of particle diameter of sample crystal phase calcined at 800 °C.

against both bacteria, but there was no sun irradiation treatment.

The quantitative test was carried out by first diluting crystal phase calcined at 700 and 800 °C in a liquid culture of nutrient broth; 1000, 500, 250, 125, 62.5, 31.25, and 15.625 µL [44]. In each tube, a bacterial suspension of 1 µL was added and followed by irradiation of sunlight for 5 min, and incubation at 37 °C for 24 h. In comparison, a similar procedure was performed on seven other tubes, but without irradiation of sunlight [45].

3. RESULTS AND DISCUSSIONS

Figure 1a shows the results of calcination at 600 °C for 15 h. Crystal phase calcined at 700 and 800 °C appeared white signifying the degradation of carbon into gases as shown in Figure 1b.

3.1. XRD Analysis

The peak results of XRD analysis for chicken eggshell powder uncalcined, crystal phase calcined at 700 and 800 °C were identified qualitatively using the Match! software as shown in Figure 2. Crystal Impact version 3.1.5 build 247 [46][47] and the National Institute of Standards and Technology Inorganic Crystal Structure Database (NIST ICSD) web application [34][48] were used. Based on the result, sample A showed a dominant crystalline phase, namely CaCO₃ with peaks at 2θ (°) of 23.22, 29.48, and 39.61, similar as reported before [49]. Similarly, crystal phase calcined at 700 and 800 °C showed multiple crystalline phases, including CaO crystal identified at 2θ (°) of 32.21, 37.37, and 53.89, consistent with a previous study [50]. Crystal

phase calcined at 800 °C also showed critical phase information of CaO at 2θ (°) of 32.31, 37.37, and 53.89, as reported in previous studies [50]. As shown in Figure 2, other crystal phases were identified, although in relatively smaller peaks. The presence of these crystalline phases was attributed to the reactions of several compounds contained in purebred chicken eggshell [27]-[29].

The analysis proceeded to the quantitative stage using the Rietica software version 4.2 Rietveld method [51], with the results presented in Table 1 and Figure 3 for chicken eggshell powder uncalcined, crystal phase calcined at 700 and 800 °C. Reference data from Crystallography Open Database (COD-96-900-9669) CIF-9009668 were used for comparison to quantitatively analyze the crystal phase of CaCO₃ from chicken eggshell powder uncalcined.

The information presented in Table 1, shows the Goodness of Fit (GoF) value of the analysis of uncalcined chicken eggshell powder of 2.61, and the Full Width Half Maximum (FWHM) value of the CaCO₃ crystal phase of 0.21 with a dominant peak of 2θ at 29.42°. where these two data are used to calculate the phase size of the crystal using the Debye Scherrer equation (1):

$$D = \frac{k \lambda}{\beta \cos \theta} \quad (1)$$

where, D = crystal phase size (nm), k = shape constant valued at 0.9–1.0, λ = X-ray wavelength used = 1.542 nm, β = Measurement result of half the maximum peak width height [52]. By using this calculation formula, the phase size of CaCO₃ crystals contained in uncalcined eggshell powder

was obtained by 277.54 nm. In addition to these data, the weight percentage of phase CaCO_3 data of 72.29 was also obtained.

Quantitative analysis of calcined eggshells at 700 °C (Table 1) informed the formation of the CaO crystalline phase. The comparison reference data used to analyze comes from COD-96-100-0045 CIF-000044 data. GoF value of 2.17 and FWHM of 0.20 with a dominant peak of 2θ at 37.99°. Using equation (1), the phase size of the CaO crystal is 41.97 nm. In addition, the weight percentage of phase CaO data was also obtained at 44.96%.

Information on the results of quantitative analysis of chicken shells calcined at 800 °C informs weight percentage of phase CaO data of 54.94%. This analysis used comparative reference data from COD-96-101-1096 CIF-000044. GoF value of 2.28 and FWHM of 0.20 with a dominant peak of 2θ at 37.47°. Using equation (1), the phase size of the CaO crystal is 41.98 nm.

The diffraction pattern shown in Figure 3a-3c shows that the diffractogram smoothing for each sample has been effectively carried out, as evidenced by the attainment of the GoF value < 4. This value was based on the difference between the observation data and the calculation results. In this case, this value was relatively small [53] reaching 2.61, 2.17, and 2.28 for chicken eggshell powder

uncalcined, crystal phase calcined at 700 and 800 °C, respectively.

3.2. FTIR Analysis

Figure 4 shows the results of FTIR analysis for chicken eggshell powder uncalcined, crystal phase calcined at 700 and 800 °C. The characteristics of chicken eggshell powder uncalcined were confirmed by the C–O functional groups with stretching observed at 1402 cm^{-1} , and a vibrating band at 880 cm^{-1} . Furthermore, a symmetric vibration band indicating Ca–O was found at a wavenumber of 715.65 cm^{-1} as previously reported by [54]. A sharp stretching band at wavenumber 3638 cm^{-1} showed the characteristics of the O–H group in $\text{Ca}(\text{OH})_2$. During the calcination process, carbonates in chicken eggshell powder uncalcined in the stretching band 1402 cm^{-1} migrated to higher energies indicating CaO, as evidenced in wavenumbers of 1446, 1059, 880, and 872 cm^{-1} , consistent with the characteristics of samples B and C [55][56].

3.3. SEM-EDS

The results of SEM-EDS analysis in Figure 5 confirm the presence of Ca, C, and O elements which show the formation of crystalline CaO in crystal phase calcined at 700 and 800 °C. SEM

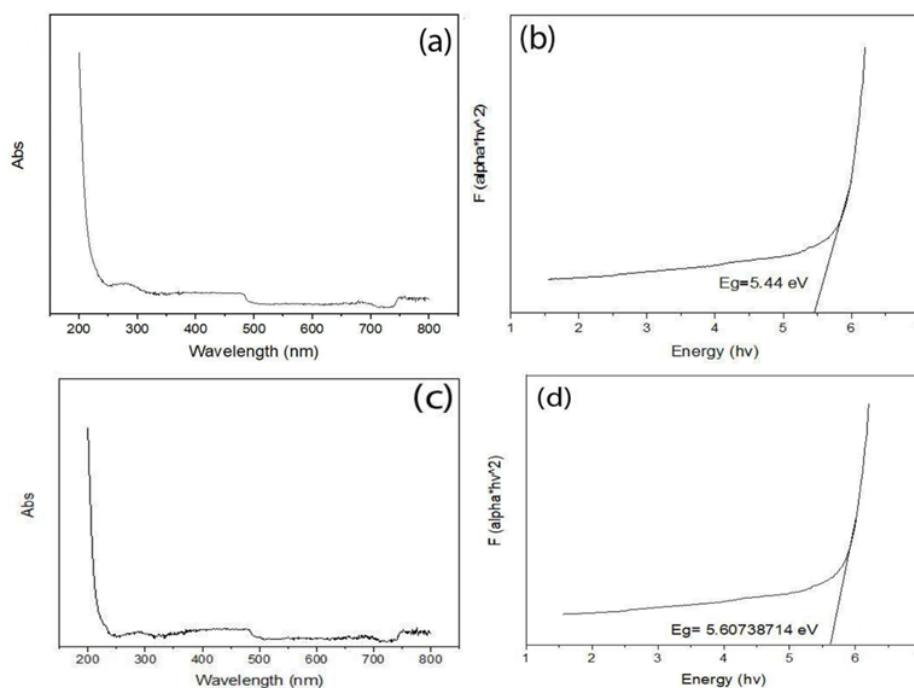


Figure 8. (a) UV light absorbance and (b) bandgap crystal phase calcined at 800 °C. (c) UV light absorbance and (d) bandgap crystal phase calcined at 700 °C.

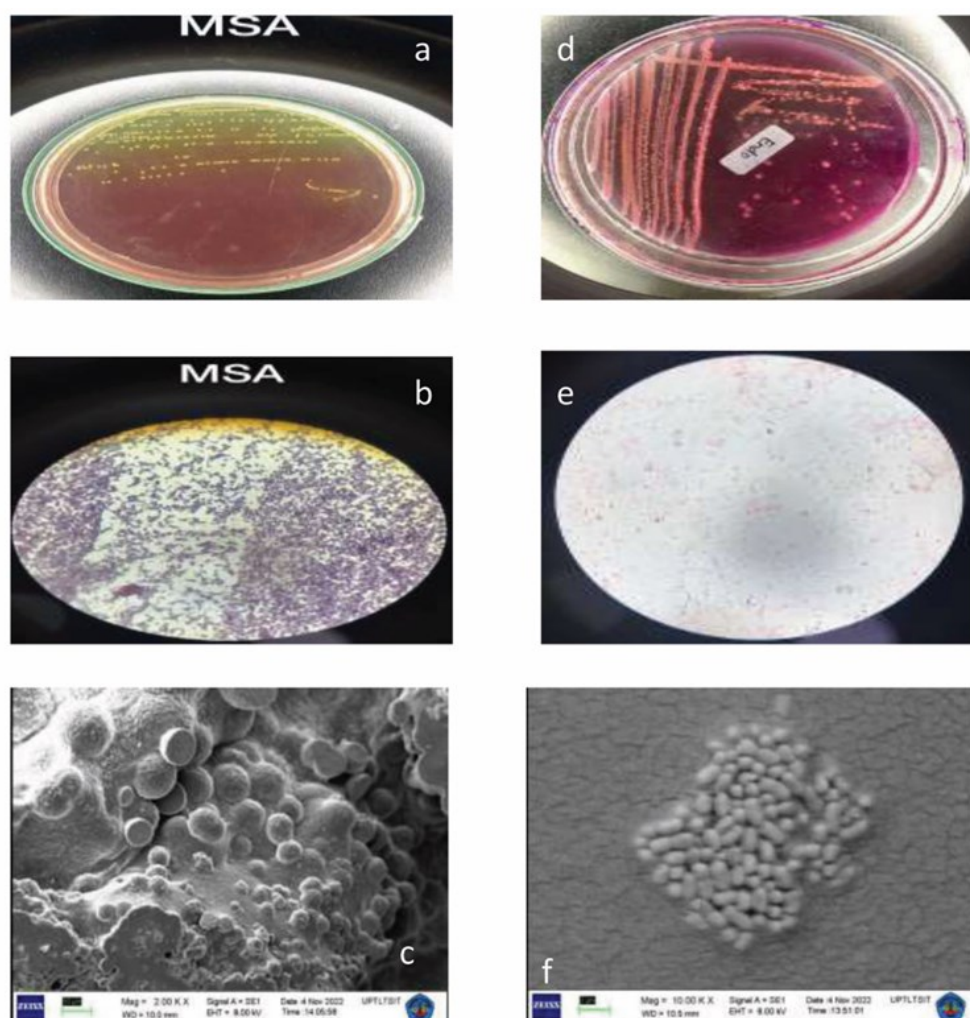


Figure 9. (a) Bacterial colonies growing on MSA cultures, (b) Gram-positive painting results from MSA cultures, (c) *S. aureus* observed in SEM magnification of 20,000x, (d) bacterial colonies growing on endo agar cultures, (e) Gram-negative painting results from endo agar culture, and (f) *E. coli* observed in SEM magnification of 20,000x.

integrated with EDS was considered useful for providing insights into the composition of the sample. X-ray was used to provide information regarding qualitative and quantitative analysis of elements present in samples. The focused electron beam interacted with the atoms in samples, providing various signals as information about the topography and composition. The energy plot (keV) of the emitted X-Ray photons (x-axis) in relation to the intensity (y-axis) of EDS spectrum showed the elemental amounts of 19.66% calcium, 28.29% carbon, and 52.05% oxygen [57].

As shown in Figure 6, SEM micrograph analysis showed that the pure chicken eggshell powder sample had a percentage porosity of 48.20% and a particle layer thickness represented by red, yellow, green, light-blue, and dark-blue colors.

Figure 6 also showed that the sample surface appeared lumpy, grainy, and irregular due to exposure to high temperatures during calcination. The formation of agglomeration showed that the crystal phase in both crystal phase calcined at 700 and 800 °C was porous due to the release of CO₂ gas during the decomposition of CaCO₃ in the calcination process. The particle size distribution was less than 20 nm (Figure 7) with a frequency of 56 as shown in the result of SEM micrograph analysis [58].

3.4. DRS-UV Analysis

The absorption spectrum of UV light for crystal phase calcined at 700 and 800 °C was scanned at wavelengths of 200–800 nm. Absorption peaks were identified at 233.017, 315.997, 516.009, and

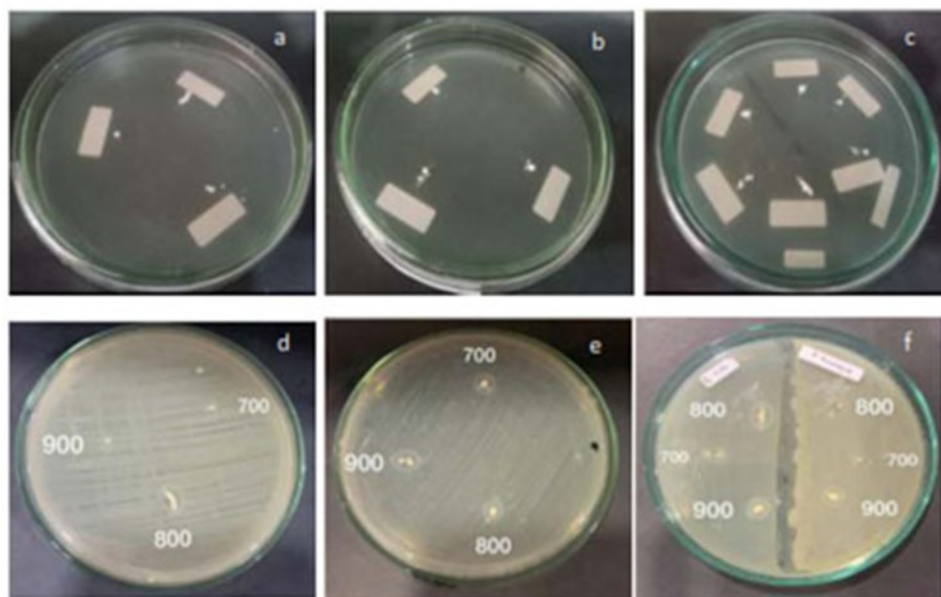


Figure 10. Test results of antibacterial activity for crystal phase calcined at 700 and 800 °C qualitatively (a, b) non-photocatalytic and (c) photocatalytic before incubation and (d, e, and f) after incubation.

741.007 nm for crystal phase calcined at 700 °C while for crystal phase calcined at 800 °C, the peaks were observed at 250.018, 332.006, and 499.908 nm. The bandgap energy was obtained with the Touc Plot method ($\alpha h\nu = A(h\nu - E_g)^{1/2}$), and the values obtained for crystal phase calcined at 700 °C were 2.07, 2.74, 3.71, and 5.96 eV. On the other hand, crystal phase calcined at 800 °C showed bandgap energies of 4.60 and 5.82 eV (Figure 8). These results agreed with previous studies [59]. The values of the energy bands for both samples affected the photoelectric effect. When irradiated by sunlight, electrons in the valence band (V_B) were excited and moved toward the conduction band (C_B). The displacement of electrons (e^-) caused the occurrence of holes denoted h^+ , while the conduction band was negatively charged because it had been occupied by e^- from the V_B [60].

3.5. Morphology of Test Bacteria

Figures 9a and 9c show that *S. aureus* colonies grown on MSA culture are visible, round, convex, small, and smooth. A visible change occurred in the culture color to yellow, showing the ability of the bacteria to ferment mannitol. The bacteria showed Gram-positive staining, were cocci-shaped, clustered, and yielded positive catalase test results. On the other hand, *E. coli* colonies inoculated in endo agar as presented in Figures 9d-9f were round, convex, small, pink, and rod-shaped, as well as

showed Gram-negative staining [61].

3.6. Bacteria Cell Death

Figure 10 shows the qualitative analysis results of MHA culture with bacteria cell death indicated by the formation of an inhibitory zone. This implies that crystal phase calcined at 700 and 800 °C can function as antibacterials. The antibacterial activity of the crystalline phase $\text{Ca}(\text{OH})_2$ occurred due to the release of hydroxyl ions in water contained in MHA cultures used for antibacterial activity assays. Hydroxyl ions (OH^-) formed the free radical species ($\bullet\text{OH}$) that acted as reactive oxidizers against various biomolecular compounds in the cell. The high reactivity of free radicals ($\bullet\text{OH}$) increases the

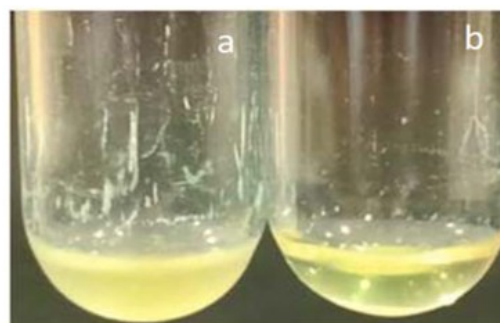


Figure 11. The results of quantitative antibacterial activity tests, (a) bacteria can grow marked by turbidity in nutrient broth cultures and (b) bacteria are unable to grow characterized by cultures that remain clear.

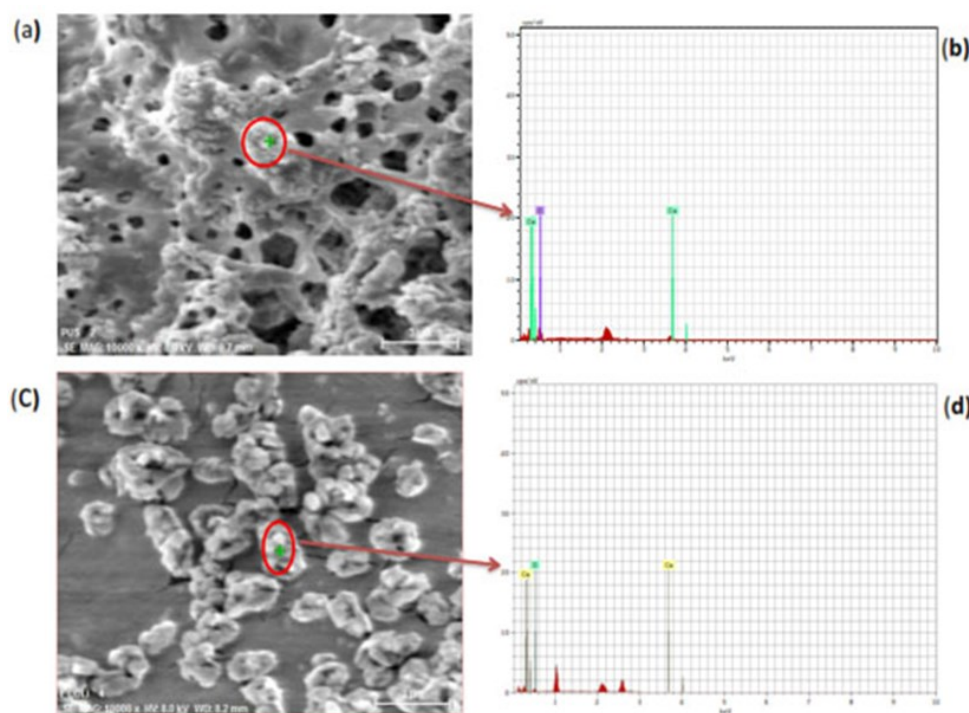


Figure 12. Results of SEM-EDS observations on *S. aureus* (a, b) and *E. coli* cell death on antibacterial activity tests (c, d).

range of diffuse areas. The impact on bacteria cell damage was attributed to several processes, namely (1) intracellular metabolic failure, (2) protein denaturation, and (3) damage to the cytoplasmic membrane [62]-[64].

As shown in Figure 11, the minimal inhibitory concentration (MIC) of purebred chicken eggshell powder containing the crystal phase was measured at 1000 μL (Fig 11b) with a marked absence of turbidity in the nutrient broth bacterial culture and also confirmed by the absence of growth after re-inoculation.

The bacterial cell death was due to the action of the CaO crystalline phase, which decomposed into Ca^{2+} ions (Figure 12). These ions interact with organic compounds on the cell wall, disrupting its permeability by interfering with bacteria cell DNA condensation [65]-[67].

3.7. Ethical Clearance

This study received approval from the Tanjungkarang Poltekkes Ethics Commission with test certificate number: 005/KEPK-TJK/X/2022.


4. CONCLUSIONS

In conclusion, this study showed the feasibility

of chicken eggshell powder as a semiconductor material through thermal decomposition. This material showed *in vitro* antibacterial activity against *S. aureus* and *E. coli* when exposed to sunlight irradiation for 5 min to achieve a photocatalyst effect. This study had certain limitations including failure to explain the mechanism of cell death. Further studies are needed to determine the effects stemming from several treatments of chicken eggshell powder. In addition, optimization of the mass, contact time, and photocatalyst energy sources other than sunlight must be further developed.

AUTHOR INFORMATION

Corresponding Author

Rudy Tahan Mangapul Situmeang —
Department of Chemistry, University of
Lampung, Bandar Lampung-35145 (Indonesia);
 orcid.org/0000-0001-6622-0362
Email: rudy.tahan@fmipa.ac.id

Authors

Rodhiansyah Djayasinga — Department of
Medical Laboratory Technology, Tanjungkarang
Health Polytechnic, Bandar Lampung-35145

(Indonesia);

 orcid.org/0000-0003-2089-0795

Fuangfa Unob — Department of Chemistry, Chulalongkorn University, Bangkok-10330 (Thailand);

 orcid.org/0000-0002-2625-9075

Sutopo Hadi — Department of Chemistry, University of Lampung, Bandar Lampung-35145 (Indonesia);

 orcid.org/0000-0001-6464-7215

Posman Manurung — Department of Physics, University of Lampung, Bandar Lampung-35145 (Indonesia);

 orcid.org/0000-0003-3484-1273

Sumardi Sumardi — Department of Biology, University of Lampung, Bandar Lampung-35145 (Indonesia);

 orcid.org/0000-0002-2773-7083

Author Contributions

Conceptualization, R. D. and R. T. M. S.; Methodology R. D., R. T. M. S., S. H., S. S.; Software R. D., P. M.; Validation, R. D., R. T. M. S., P. M., F.U; Formal Analysis R. D., R. T. M. S., P. M., S. H., F. U; Resources R. D., P. M., F. U; Data Curation R. D.; Writing – Original Draft Preparation, R. D.; Writing – Review & Editing R. T. M. S., PGM., F. U; Visualization R. T. M. S., P. M.; Supervision R. T. M. S., P. M., S. H., S. S., F. U; Project Administration R. D.; Funding Acquisition, R. D.

Conflicts of Interest

The authors declare no conflict of interest.

ACKNOWLEDGEMENT

We would like to thank all parties who have supported the implementation of this research, especially the Tanjungkarang Health Polytechnic of the Ministry of Health of the Republic of Indonesia through the Decree of the Director of the Tanjungkarang Health Polytechnic Number: HK.02.03/1.2/32/2022 and to the University of Lampung through the HETI (Higher Education for Technology and Innovation) Program.

REFERENCES

- [1] M. E. S. Sule, E. Astuty, and R. Tahitu. (2023). "In Vitro Antibacterial Activity and Phytochemical Screening of Galoba (*Hornstedtia alliacea*) Seeds Extract". *Bioactivities*. **1** (2): 81-89. [10.47352/bioactivities.2963-654X.196](https://doi.org/10.47352/bioactivities.2963-654X.196).
- [2] S. A. Polash, T. Khare, V. Kumar, and R. Shukla. (2021). "Prospects of Exploring the Metal-Organic Framework for Combating Antimicrobial Resistance". *ACS Applied Bio Materials*. **4** (12): 8060-8079. [10.1021/acsabm.1c00832](https://doi.org/10.1021/acsabm.1c00832).
- [3] Y. S. Kurniawan, T. Indriani, H. Amrulloh, L. C. Adi, A. C. Imawan, K. T. A. Priyanga, and E. Yudha. (2023). "Journey of Natural Products: From Isolation Stage to Drug's Approval in Clinical Trials". *Bioactivities*. **1** (2): 43-60. [10.47352/bioactivities.2963-654X.190](https://doi.org/10.47352/bioactivities.2963-654X.190).
- [4] J. W. Betts, M. Hornsey, and R. M. La Ragione. (2018). "Novel Antibacterials: Alternatives to Traditional Antibiotics". *Advances in Microbial Physiology*. **73** : 123-169. [10.1016/bs.ampbs.2018.06.001](https://doi.org/10.1016/bs.ampbs.2018.06.001).
- [5] A. Valsamatzi-Panagiotou, M. Traykovska, and R. Penchovsky. (2020). In: "Drug Discovery Targeting Drug-Resistant Bacteria". 9-37. [10.1016/b978-0-12-818480-6.00002-3](https://doi.org/10.1016/b978-0-12-818480-6.00002-3).
- [6] T. N. Almanaa, S. A. Alyahya, J. M. Khaled, M. R. Shehu, N. S. Alharbi, S. Kadaikunnan, A. S. Alobaidi, and A. Khalid Alzahrani. (2020). "The extreme drug resistance (XDR) *Staphylococcus aureus* strains among patients: A retrospective study". *Saudi Journal of Biological Sciences*. **27** (8): 1985-1992. [10.1016/j.sjbs.2020.04.003](https://doi.org/10.1016/j.sjbs.2020.04.003).
- [7] M. Koeck, K. Como-Sabetti, D. Boxrud, G. Dobbins, A. Glennen, M. Anacker, S. Jawahir, I. See, and R. Lynfield. (2019). "Burdens of Invasive Methicillin-Susceptible and Methicillin-Resistant *Staphylococcus aureus* Disease, Minnesota, USA". *Emerging Infectious Diseases*. **25** (1): 171-174. [10.3201/eid2501.181146](https://doi.org/10.3201/eid2501.181146).
- [8] M. Brown-Jaque, W. Calero-Caceres, and M.

- Muniesa. (2015). "Transfer of antibiotic-resistance genes via phage-related mobile elements". *Plasmid*. **79** : 1-7. [10.1016/j.plasmid.2015.01.001](https://doi.org/10.1016/j.plasmid.2015.01.001).
- [9] A. Karkman, T. T. Do, F. Walsh, and M. P. J. Virta. (2018). "Antibiotic-Resistance Genes in Waste Water". *Trends in Microbiology*. **26** (3): 220-228. [10.1016/j.tim.2017.09.005](https://doi.org/10.1016/j.tim.2017.09.005).
- [10] S. R. Partridge, S. M. Kwong, N. Firth, and S. O. Jensen. (2018). "Mobile Genetic Elements Associated with Antimicrobial Resistance". *Clinical Microbiology Reviews*. **31** (4). [10.1128/CMR.00088-17](https://doi.org/10.1128/CMR.00088-17).
- [11] P. G. Bhavyasree and T. S. Xavier. (2020). "Green synthesis of Copper Oxide/Carbon nanocomposites using the leaf extract of Adhatoda vasica Nees, their characterization and antimicrobial activity". *Heliyon*. **6** (2): e03323. [10.1016/j.heliyon.2020.e03323](https://doi.org/10.1016/j.heliyon.2020.e03323).
- [12] C. Mallikarjunaswamy, J. S. Vidya, H. N. Deepakumari, G. Nagaraju, M. A. Sangamesha, and V. Lakshmi Ranganatha. (2022). "Larvicidal and antimicrobial activity of zinc oxide nanoparticles synthesized from rain tree pod aqueous extract". *Materials Today: Proceedings*. **62** : 5083-5086. [10.1016/j.matpr.2022.02.422](https://doi.org/10.1016/j.matpr.2022.02.422).
- [13] A. Nigam, S. Saini, B. Singh, A. K. Rai, and S. J. Pawar. (2022). "Zinc doped magnesium ferrite nanoparticles for evaluation of biological properties viz antimicrobial, biocompatibility, and in vitro cytotoxicity". *Materials Today Communications*. **31**. [10.1016/j.mtcomm.2022.103632](https://doi.org/10.1016/j.mtcomm.2022.103632).
- [14] S. Zhang, L. Lin, X. Huang, Y.-G. Lu, D.-L. Zheng, Y. Feng, and L. Balan. (2022). "Antimicrobial Properties of Metal Nanoparticles and Their Oxide Materials and Their Applications in Oral Biology". *Journal of Nanomaterials*. **2022** : 1-18. [10.1155/2022/2063265](https://doi.org/10.1155/2022/2063265).
- [15] M. E. Abdel-Alim, K. Samaan, D. Guillaume, and H. Amla. (2023). "Green Synthesis of Silver Nanoparticles using Egyptian Date Palm (Phoenix dactylifera L.) Seeds and Their Antibacterial Activity Assessment". *Bioactivities*. **1** (1): 1-8. [10.47352/bioactivities.2963-654X.180](https://doi.org/10.47352/bioactivities.2963-654X.180).
- [16] Z. Kolenc, T. Langerholc, G. Hostnik, M. Ocvirk, S. Stumpf, M. Pintaric, I. J. Kosir, A. Cerenak, A. Garmut, and U. Bren. (2022). "Antimicrobial Properties of Different Hop (*Humulus lupulus*) Genotypes". *Plants (Basel)*. **12** (1). [10.3390/plants12010120](https://doi.org/10.3390/plants12010120).
- [17] K. Sak. (2023). "Role of Flavonoids as Potential Plant Fungicides in Preventing Human Carcinogenesis: A Short Communication". *Bioactivities*. **1** (2): 39-42. [10.47352/bioactivities.2963-654X.187](https://doi.org/10.47352/bioactivities.2963-654X.187).
- [18] J. Gomez-Estaca, A. Aleman, M. E. Lopez-Caballero, G. C. Baccan, P. Montero, and M. C. Gomez-Guillen. (2019). "Bioaccessibility and antimicrobial properties of a shrimp demineralization extract blended with chitosan as wrapping material in ready-to-eat raw salmon". *Food Chemistry*. **276** : 342-349. [10.1016/j.foodchem.2018.10.031](https://doi.org/10.1016/j.foodchem.2018.10.031).
- [19] V. C. Amador, C. A. D. Santos-Silva, L. M. B. Vilela, M. Oliveira-Lima, M. de Santana Rego, R. S. Roldan-Filho, R. L. Oliveira-Silva, A. B. Lemos, W. D. de Oliveira, J. R. C. Ferreira-Neto, S. Crovella, and A. M. Benko-Iseppon. (2021). "Lipid Transfer Proteins (LTPs)-Structure, Diversity and Roles beyond Antimicrobial Activity". *Antibiotics (Basel)*. **10** (11). [10.3390/antibiotics10111281](https://doi.org/10.3390/antibiotics10111281).
- [20] B. Shang, S. Wang, L. Lu, H. Ma, A. Liu, A. Zupanic, L. Jiang, A. S. Elnawawy, and Y. Yu. (2022). "Poultry eggshell-derived antimicrobial materials: Current status and future perspectives". *Journal of Environmental Management*. **314** : 115096. [10.1016/j.jenvman.2022.115096](https://doi.org/10.1016/j.jenvman.2022.115096).
- [21] A. Jayakumar, S. Radoor, J. Karayil, I. C. Nair, S. Siengchin, J. Parameswaranpillai, and E. K. Radhakrishnan. (2022). In: "Polymer Based Bio-nanocomposites, Composites Science, and Technology". 87-102. [10.1007/978-981-16-8578-1_5](https://doi.org/10.1007/978-981-16-8578-1_5).
- [22] H. Salazar, P. M. Martins, B. Santos, M. M. Fernandes, A. Reizabal, V. Sebastian, G. Botelho, C. J. Tavares, J. L. Vilas-Vilela, and S. Lanceros-Mendez. (2020). "Photocatalytic and antimicrobial multifunctional

- nanocomposite membranes for emerging pollutants water treatment applications". *Chemosphere*. **250** : 126299. [10.1016/j.chemosphere.2020.126299](https://doi.org/10.1016/j.chemosphere.2020.126299).
- [23] S. Sharifi, A. Zaheri Khosroshahi, S. Maleki Dizaj, and Y. Rezaei. (2021). "Preparation, Physicochemical Assessment and the Antimicrobial Action of Hydroxyapatite-Gelatin/Curcumin Nanofibrous Composites as a Dental Biomaterial". *Biomimetics (Basel)*. **7** (1). [10.3390/biomimetics7010004](https://doi.org/10.3390/biomimetics7010004).
- [24] B. Liu, L. Mu, J. Zhang, X. Han, and H. Shi. (2020). "TiO₂/Cu₂(OH)₂CO₃ nanocomposite as efficient antimicrobials for inactivation of crop pathogens in agriculture". *Materials Science & Engineering C-Materials for Biological Applications*. **107** : 110344. [10.1016/j.msec.2019.110344](https://doi.org/10.1016/j.msec.2019.110344).
- [25] L. Motelica, D. Fica, A. Fica, R. D. Trusca, C. I. Ilie, O. C. Oprea, and E. Andronescu. (2020). "Innovative Antimicrobial Chitosan/ZnO/Ag NPs/Citronella Essential Oil Nanocomposite-Potential Coating for Grapes". *Foods*. **9** (12). [10.3390/foods9121801](https://doi.org/10.3390/foods9121801).
- [26] R. Amanda Firza, A. Ulfah, and S. Slamet. (2020). "Antibacterial activity of CaO from blood cockle shells (*Anadara granosa*) calcination against *Escherichia coli*". *Biodiversitas Journal of Biological Diversity*. **21** (6). [10.13057/biodiv/d210660](https://doi.org/10.13057/biodiv/d210660).
- [27] S. Aina, B. D. Plessis, V. Mjimba, and H. Brink. (2021). "Eggshell Valorization: Membrane Removal, Calcium Oxide Synthesis, and Biochemical Compound Recovery towards Cleaner Productions". *Biointerface Research in Applied Chemistry*. **12** (5): 5870-5883. [10.33263/briac125.58705883](https://doi.org/10.33263/briac125.58705883).
- [28] E. M. Rivera, M. Araiza, W. Brostow, V. M. Castaño, J. R. Díaz-Estrada, R. Hernández, and J. R. Rodríguez. (1999). "Synthesis of hydroxyapatite from eggshells". *Materials Letters*. **41** (3): 128-134. [10.1016/s0167-577x\(99\)00118-4](https://doi.org/10.1016/s0167-577x(99)00118-4).
- [29] Y. S. Ok, S. S. Lee, W. T. Jeon, S. E. Oh, A. R. Usman, and D. H. Moon. (2011). "Application of eggshell waste for the immobilization of cadmium and lead in a contaminated soil". *Environmental Geochemistry and Health*. **33 Suppl 1** : 31-9. [10.1007/s10653-010-9362-2](https://doi.org/10.1007/s10653-010-9362-2).
- [30] F. Antolini, E. Burrelli, L. Stroea, V. Morandi, L. Ortolani, G. Accorsi, and M. Blosi. (2012). "Time and Temperature Dependence of CdS Nanoparticles Grown in a Polystyrene Matrix". *Journal of Nanomaterials*. **2012** : 1-11. [10.1155/2012/815696](https://doi.org/10.1155/2012/815696).
- [31] K. Berent, S. Komarek, R. Lach, and W. Pyda. (2019). "The Effect of Calcination Temperature on the Structure and Performance of Nanocrystalline Mayenite Powders". *Materials (Basel)*. **12** (21). [10.3390/ma12213476](https://doi.org/10.3390/ma12213476).
- [32] A. K. Kushwaha, M. John, M. Misra, and P. L. Menezes. (2021). "Nanocrystalline Materials: Synthesis, Characterization, Properties, and Applications". *Crystals*. **11** (11). [10.3390/cryst11111317](https://doi.org/10.3390/cryst11111317).
- [33] L. K. Varga, É. Bakos, É. Kisdi-Koszó, É. Zsoldos, and L. F. Kiss. (1994). "Time and temperature dependence of nanocrystalline structure formation in a Finemet-type amorphous alloy". *Journal of Magnetism and Magnetic Materials*. **133** (1-3): 280-282. [10.1016/0304-8853\(94\)90546-0](https://doi.org/10.1016/0304-8853(94)90546-0).
- [34] R. Mohadi, K. Anggraini, F. Riyanti, and A. Lesbani. (2016). "Preparation Calcium Oxide From Chicken Eggshells". *Sriwijaya Journal of Environment*. **1** (2): 32-35. [10.22135/sje.2016.1.2.32-35](https://doi.org/10.22135/sje.2016.1.2.32-35).
- [35] M. Ambrosi, L. Dei, R. Giorgi, C. Neto, and P. Baglioni. (2001). "Colloidal Particles of Ca(OH)₂: Properties and Applications to Restoration of Frescoes". *Langmuir*. **17** (14): 4251-4255. [10.1021/la010269b](https://doi.org/10.1021/la010269b).
- [36] Z. Mirghiasi, F. Bakhtiari, E. Darezereshki, and E. Esmaeilzadeh. (2014). "Preparation and characterization of CaO nanoparticles from Ca(OH)₂ by direct thermal decomposition method". *Journal of Industrial and Engineering Chemistry*. **20** (1): 113-117. [10.1016/j.jiec.2013.04.018](https://doi.org/10.1016/j.jiec.2013.04.018).

- [37] S. Molinari, B. Swinyard, J. Bally, M. Barlow, J. P. Bernard, P. Martin, T. Moore, A. Noriega-Crespo, R. Plume, L. Testi, A. Zavagno, A. Abergel, B. Ali, P. André, J. P. Baluteau, M. Benedettini, O. Berné, N. P. Billot, J. Blommaert, S. Bontemps, F. Boulanger, J. Brand, C. Brunt, M. Burton, L. Campeggio, S. Carey, P. Caselli, R. Cesaroni, J. Cernicharo, S. Chakrabarti, A. Chrysostomou, C. Codella, M. Cohen, M. Compiegne, C. J. Davis, P. de Bernardis, G. de Gasperis, J. Di Francesco, A. M. di Giorgio, D. Elia, F. Faustini, J. F. Fischera, Y. Fukui, G. A. Fuller, K. Ganga, P. Garcia-Lario, M. Giard, G. Giardino, J. Glenn, P. Goldsmith, M. Griffin, M. Hoare, M. Huang, B. Jiang, C. Joblin, G. Joncas, M. Juvela, J. Kirk, G. Lagache, J. Z. Li, T. L. Lim, S. D. Lord, P. W. Lucas, B. Maiolo, M. Marengo, D. Marshall, S. Masi, F. Massi, M. Matsuura, C. Meny, V. Minier, M. A. Miville-Deschênes, L. Montier, F. Motte, T. G. Müller, P. Natoli, J. Neves, L. Olmi, R. Paladini, D. Paradis, M. Pestalozzi, S. Pezzuto, F. Piacentini, M. Pomarès, C. C. Popescu, W. T. Reach, J. Richer, I. Ristorcelli, A. Roy, P. Royer, D. Russeil, P. Saraceno, M. Sauvage, P. Schilke, N. Schneider-Bontemps, F. Schuller, B. Schultz, D. S. Shepherd, B. Sibthorpe, H. A. Smith, M. D. Smith, L. Spinoglio, D. Stamatellos, F. Strafella, G. Stringfellow, E. Sturm, R. Taylor, M. A. Thompson, R. J. Tuffs, G. Umana, L. Valenziano, R. Vavrek, S. Viti, C. Waelkens, D. Ward-Thompson, G. White, F. Wyrowski, H. W. Yorke and Q. Zhang. (2010). "Hi-GAL: The Herschel Infrared Galactic Plane Survey". *Publications of the Astronomical Society of the Pacific*. **122** (889): 314-325. [10.1086/651314](https://doi.org/10.1086/651314).
- [38] N. Razali, M. A. Azizan, K. F. Pa'ee, N. Razali, and N. Jumadi. (2020). "Preliminary studies on calcinated chicken eggshells as fine aggregates replacement in conventional concrete". *Materials Today: Proceedings*. **31** : 354-359. [10.1016/j.matpr.2020.06.232](https://doi.org/10.1016/j.matpr.2020.06.232).
- [39] A. Giacometti, O. Cirioni, F. Barchiesi, M. S. Del Prete, M. Fortuna, F. Caselli, and G. Scalise. (2000). "In vitro susceptibility tests for cationic peptides: comparison of broth microdilution methods for bacteria that grow aerobically". *Antimicrobial Agents and Chemotherapy*. **44** (6): 1694-6. [10.1128/AAC.44.6.1694-1696.2000](https://doi.org/10.1128/AAC.44.6.1694-1696.2000).
- [40] E. Nagy, L. Boyanova, U. S. Justesen, and E. S. G. o. A. Infections. (2018). "How to isolate, identify and determine antimicrobial susceptibility of anaerobic bacteria in routine laboratories". *Clinical Microbiology and Infection*. **24** (11): 1139-1148. [10.1016/j.cmi.2018.02.008](https://doi.org/10.1016/j.cmi.2018.02.008).
- [41] S. Ahmad Bhat, F. Zafar, A. Ullah Mirza, A. Hossain Mondal, A. Kareem, Q. Mohd. Rizwanul Haq, and N. Nishat. (2020). "NiO nanoparticle doped-PVA-MF polymer nanocomposites: Preparation, Congo red dye adsorption and antibacterial activity". *Arabian Journal of Chemistry*. **13** (6): 5724-5739. [10.1016/j.arabjc.2020.04.011](https://doi.org/10.1016/j.arabjc.2020.04.011).
- [42] A. W. Bauer, W. M. M. Kirby, J. C. Sherris, and M. Turck. (1966). "Antibiotic Susceptibility Testing by a Standardized Single Disk Method". *American Journal of Clinical Pathology*. **45** (4_ts): 493-496. [10.1093/ajcp/45.4_ts.493](https://doi.org/10.1093/ajcp/45.4_ts.493).
- [43] M. Ikram, T. Inayat, A. Haider, A. Ul-Hamid, J. Haider, W. Nabgan, A. Saeed, A. Shahbaz, S. Hayat, K. Ul-Ain, and A. R. Butt. (2021). "Graphene Oxide-Doped MgO Nanostructures for Highly Efficient Dye Degradation and Bactericidal Action". *Nanoscale Research Letters*. **16** (1): 56. [10.1186/s11671-021-03516-z](https://doi.org/10.1186/s11671-021-03516-z).
- [44] L. Cai, J. Chen, Z. Liu, H. Wang, H. Yang, and W. Ding. (2018). "Magnesium Oxide Nanoparticles: Effective Agricultural Antibacterial Agent Against *Ralstonia solanacearum*". *Frontiers in Microbiology*. **9** : 790. [10.3389/fmicb.2018.00790](https://doi.org/10.3389/fmicb.2018.00790).
- [45] F. Mohamed, M. Shaban, G. Aljohani, and A. M. Ahmed. (2021). "Synthesis of novel eco-friendly CaO/C photocatalyst from coffee and eggshell wastes for dye degradation". *Journal of Materials Research*

- and Technology. **14** : 3140-3149. [10.1016/j.jmrt.2021.08.055](https://doi.org/10.1016/j.jmrt.2021.08.055).
- [46] I. Levin. *NIST Inorganic Crystal Structure Database (ICSD)*. [10.18434/M32147](https://doi.org/10.18434/M32147).
- [47] N. R. Elejalde-Cadena, J. O. Estevez, V. Torres-Costa, M. D. Ynsa-Alcalá, G. García-López, and A. Moreno. (2021). "Molecular Analysis of the Mineral Phase and Examination of Possible Intramineral Proteins of Dinosaur Eggshells Collected in El Rosario, Baja California, Mexico". *ACS Earth and Space Chemistry*. **5** (6): 1552-1563. [10.1021/acsearthspacechem.1c00077](https://doi.org/10.1021/acsearthspacechem.1c00077).
- [48] D. Xidaki, P. Agrafioti, D. Diomatari, A. Kaminari, E. Tsalavoutas-Psarras, P. Alexiou, V. Psycharis, E. C. Tsilibary, S. Silvestros, and M. Sagnou. (2018). "Synthesis of Hydroxyapatite, beta-Tricalcium Phosphate and Biphasic Calcium Phosphate Particles to Act as Local Delivery Carriers of Curcumin: Loading, Release and In Vitro Studies". *Materials (Basel)*. **11** (4). [10.3390/ma11040595](https://doi.org/10.3390/ma11040595).
- [49] H. Sitepu, B. H. O'Connor, and D. Li. (2005). "Comparative evaluation of the March and generalized spherical harmonic preferred orientation models using X-ray diffraction data for molybdenite and calcite powders". *Journal of Applied Crystallography*. **38** (1): 158-167. [10.1107/s0021889804031231](https://doi.org/10.1107/s0021889804031231).
- [50] W. Primak, H. Kaufman, and R. Ward. (2002). "X-Ray Diffraction Studies of Systems Involved in the Preparation of Alkaline Earth Sulfide and Selenide Phosphors". *Journal of the American Chemical Society*. **70** (6): 2043-2046. [10.1021/ja01186a018](https://doi.org/10.1021/ja01186a018).
- [51] M. M. Hasan, E. Kisi, and H. Sugo. (2021). "Synthesis of nanostructured lanthanum hexaboride via simple borothermal routes at low temperatures". *Ceramics International*. **47** (20): 29295-29302. [10.1016/j.ceramint.2021.07.094](https://doi.org/10.1016/j.ceramint.2021.07.094).
- [52] R. Situmeang, R. Supryanto, L. N. Albert Kahar, W. Simanjuntak, and S. Sembiring. (2017). "Characteristics of Nano-Size LaCrO₃ Prepared Through Sol-Gel Route Using Pectin as Emulsifying Agent". *Oriental Journal of Chemistry*. **33** (04): 1705-1713. [10.13005/ojc/330415](https://doi.org/10.13005/ojc/330415).
- [53] C. Dong. (1999). "PowderX: Windows-95-based program for powder X-ray diffraction data processing". *Journal of Applied Crystallography*. **32** (4): 838-838. [10.1107/s0021889899003039](https://doi.org/10.1107/s0021889899003039).
- [54] B. Maringgal, N. Hashim, I. S. M. A. Tawakkal, M. H. Hamzah, and M. T. M. Mohamed. (2020). "Biosynthesis of CaO nanoparticles using Trigona sp. Honey: Physicochemical characterization, antifungal activity, and cytotoxicity properties". *Journal of Materials Research and Technology*. **9** (5): 11756-11768. [10.1016/j.jmrt.2020.08.054](https://doi.org/10.1016/j.jmrt.2020.08.054).
- [55] M. L. Granados, M. D. Z. Poves, D. M. Alonso, R. Mariscal, F. C. Galisteo, R. Moreno-Tost, J. Santamaría, and J. L. G. Fierro. (2007). "Biodiesel from sunflower oil by using activated calcium oxide". *Applied Catalysis B: Environmental*. **73** (3-4): 317-326. [10.1016/j.apcatb.2006.12.017](https://doi.org/10.1016/j.apcatb.2006.12.017).
- [56] M. Kirubakaran and V. Arul Mozhi Selvan. (2021). "Experimental investigation on the effects of micro eggshell and nano-eggshell catalysts on biodiesel optimization from waste chicken fat". *Bioresource Technology Reports*. **14**. [10.1016/j.biteb.2021.100658](https://doi.org/10.1016/j.biteb.2021.100658).
- [57] H. A. Jaber, R. S. Mahdi, and A. K. Hassan. (2020). "Influence of eggshell powder on the Portland cement mortar properties". *Materials Today: Proceedings*. **20** : 391-396. [10.1016/j.matpr.2019.09.153](https://doi.org/10.1016/j.matpr.2019.09.153).
- [58] K. Khairurrijal and M. Abdullah. (2016). "A Simple Method for Determining Surface Porosity Based on SEM Images Using OriginPro Software". *Indonesian Journal of Physics*. **20** (2): 37-40. [10.5614/itb.iip.2009.20.2.4](https://doi.org/10.5614/itb.iip.2009.20.2.4).
- [59] K. K. Jaiswal, S. Dutta, C. B. Pohrmen, R. Verma, A. Kumar, and A. P. Ramaswamy. (2020). "Bio-waste chicken eggshell-derived calcium oxide for photocatalytic application in methylene blue dye degradation under natural sunlight irradiation". *Inorganic and Nano-Metal Chemistry*. **51** (7): 995-1004. [10.1080/24701556.2020.1813769](https://doi.org/10.1080/24701556.2020.1813769).

- [60] X. Yang and D. Wang. (2018). "Photocatalysis: From Fundamental Principles to Materials and Applications". *ACS Applied Energy Materials*. **1** (12): 6657-6693. [10.1021/acsaem.8b01345](https://doi.org/10.1021/acsaem.8b01345).
- [61] M. Vaneechoutte, L. Dijkshoorn, A. Nemec, P. Kampf, and G. Wauters. (2011). In: "Manual of Clinical Microbiology". 714-738. [10.1128/9781555816728.ch42](https://doi.org/10.1128/9781555816728.ch42).
- [62] W. W. Navarre and O. Schneewind. (1994). "Proteolytic cleavage and cell wall anchoring at the LPXTG motif of surface proteins in gram-positive bacteria". *Molecular Microbiology*. **14** (1): 115-21. [10.1111/j.1365-2958.1994.tb01271.x](https://doi.org/10.1111/j.1365-2958.1994.tb01271.x).
- [63] W. W. Navarre and O. Schneewind. (1999). "Surface proteins of gram-positive bacteria and mechanisms of their targeting to the cell wall envelope". *Microbiology and Molecular Biology Reviews*. **63** (1): 174-229. [10.1128/MMBR.63.1.174-229.1999](https://doi.org/10.1128/MMBR.63.1.174-229.1999).
- [64] L. Chávez Guerrero, J. Garza-Cervantes, D. Caballero-Hernández, R. González-López, S. Sepúlveda-Guzmán, and E. Cantú-Cárdenas. (2017). "Synthesis and Characterization of Calcium Hydroxide Obtained from Agave Bagasse and Investigation of Its Antibacterial Activity". *Revista Internacional de Contaminación Ambiental*. **33** (2): 347-353. [10.20937/rica.2017.33.02.15](https://doi.org/10.20937/rica.2017.33.02.15).
- [65] G. Jin, H. Qin, H. Cao, S. Qian, Y. Zhao, X. Peng, X. Zhang, X. Liu, and P. K. Chu. (2014). "Synergistic effects of dual Zn/Ag ion implantation in osteogenic activity and antibacterial ability of titanium". *Biomaterials*. **35** (27): 7699-7713. [10.1016/j.biomaterials.2014.05.074](https://doi.org/10.1016/j.biomaterials.2014.05.074).
- [66] R. Kaliyaperumal, V. K. Poovan, and P. Shanmugam. (2023). "Synthesis and antimicrobial activity of CuO@BaO/CaO nanocomposites using precipitation method". *Journal of the Indian Chemical Society*. **100** (1). [10.1016/j.jics.2022.100842](https://doi.org/10.1016/j.jics.2022.100842).
- [67] X. Zhang, M. Liu, Z. Kang, B. Wang, B. Wang, F. Jiang, X. Wang, D.-P. Yang, and R. Luque. (2020). "NIR-triggered photocatalytic/photothermal/photodynamic water remediation using eggshell-derived CaCO₃/CuS nanocomposites". *Chemical Engineering Journal*. **388**. [10.1016/j.cej.2020.124304](https://doi.org/10.1016/j.cej.2020.124304).